IL NUOVO CIMENTO **47 C** (2024) 181
DOI 10.1393/ncc/i2024-24181-1

COLLOQUIA: HADRON2023

Search for exotic hadrons in $\eta^{(\prime)}\pi$ at GlueX

M. ALBRECHT for the GLUEX COLLABORATION

Thomas Jefferson National Accelerator Facility - 12000 Jefferson Avenue, Newport News, VA 23606, USA

received 21 December 2023

Summary. — The theoretical description of the strong interaction between quarks and gluons that form hadrons is provided by quantum chromodynamics. However, the impact of gluonic excitations on the characteristics of hadrons and their role in hadronic structure is yet to be determined. Recent discoveries of several possibly exotic hadrons highlight the significance of spectroscopic measurements in comprehending the nature of the strong interaction. These proceedings focus on the status of the hunt for exotic contributions in photoproduction data obtained with the GlueX experiment at Jefferson Lab in $\eta(')\pi$ systems. Specifically, we discuss the investigation of the $a_2(1320)$ meson production in these key channels, which is an initial step towards identifying exotic quantum-number states, where gluonic excitations contribute to the external properties, called hybrid states. Furthermore, the discussion will cover the application of an amplitude analysis that exploits the polarization of the photon beam available to the GlueX experiment and its implications for identifying the lightest hybrid meson.

1. – Introduction

The GlueX experiment is a photoproduction experiment utilizing a linearly polarized and energy tagged photon beam in Hall-D at the Thomas Jefferson National Accelerator facility in Newport News, VA. One of the main goals of the GlueX physics program is to map out the spectrum of light-quark hybrid mesons, which have been predicted in Lattice QCD calculations [1]. The GlueX detector and beamline are described elsewhere [2] and in these proceedings [3]. An important aspect of the detector system for the analyses described here are the capabilities for detection and reconstruction of charged and neutral particles in almost the full solid angle around the liquid hydrogen target.

Various experimental investigations have been conducted to probe the decays of potential hybrid mesons into final states like $\eta\pi$ and $\eta'\pi$. A noteworthy advantage of the $\eta^{(')}\pi$ systems lies in the inherent emergence of exotic quantum numbers (J^{PC}) when the system is observed in a state with odd orbital angular momentum. These distinct quantum numbers are unreachable for a conventional meson ($q\overline{q}$) state [4]. Recently,

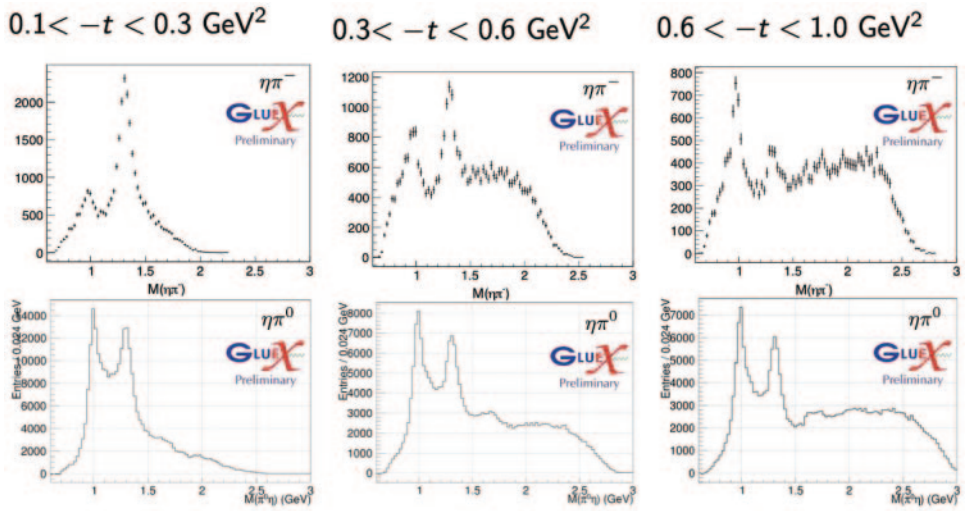

Fig. 1. – Invariant mass spectrum of the $\eta\pi^-$ (top) and $\eta\pi^0$ (bottom) systems in three bins of momentum transfer t from GlueX-I data after background subtraction (not corrected for acceptance) showing clear signals at the masses corresponding to the $a_0(980)$ and $a_2(1320)$ mesons.

the Joint Physics Analysis Center (JPAC) Collaboration determined the resonance pole parameters for the lightest hybrid state, the $\pi_1(1600)$, using a coupled channel analysis of COMPASS data for the $\eta\pi$ and $\eta'\pi$ final states [5]. The GlueX experiment aims to measure the spin-exotic contribution in these two-pseudoscalar final states in photoproduction and determine the pole positions of resonant contributions.

We are establishing the fundamental framework for investigating hybrid mesons in photoproduction through the analysis of the process $a_2 \to \eta\pi$. Specifically, we focus on the $a_2(1320)$ production in dependance of the momentum transfer t. A comprehensive understanding of the production dynamics of the well-established a_2 meson is crucial for the accurate identification of hybrid states decaying into $\eta^{(\prime)}\pi$ final states. Figure 1 shows the reconstructed GlueX data for the neutral and charged $\eta\pi$ final states after background rejection in three regions of momentum transfer t. Two clear signals at the masses corresponsing to the $a_0(980)$ and $a_2(1320)$ mesons are clearly visible. The figure illustrates the evolution of these two distinct signals with momentum transfer and motivates the detailed investigation using an amplitude analysis which will also exploit the photon polarization.

2. – Results

GlueX has performed measurements of beam asymmetries to investigate the production mechanism of single pseudoscalar mesons [6-9]. Additionally, efforts are underway to extract Spin Density Matrix Elements (SDMEs) to assess vector meson production [10]. As a next step, we focus on examining the production mechanism for established mesons, like the a_0 and a_2, which decay into $\eta\pi$ final states utilizing an amplitude analysis. Firstly, we employed a fully mass-independent approach and analysed the data in bins of the invariant $\eta\pi$ mass to extract relative strengths of various contributing waves. We make

use of polarized photoproduction amplitudes developed by JPAC [11]. The intensity is given by

$$I(\Omega,\Phi) = 2\kappa \sum_k \Bigg((1-P_\gamma)\Bigg[\sum_{l,m}[l]^{(-)}_{m;k}\Re[Z^m_l(\Omega,\Phi)]\Bigg]^2 + (1-P_\gamma)\Bigg[\sum_{l,m}[l]^{(+)}_{m;k}\Im[Z^m_l(\Omega,\Phi)]\Bigg]^2 + (1+P_\gamma)\Bigg[\sum_{l,m}[l]^{(+)}_{m;k}\Re[Z^m_l(\Omega,\Phi)]\Bigg]^2 + (1+P_\gamma)\Bigg[\sum_{l,m}[l]^{(-)}_{m;k}\Im[Z^m_l(\Omega,\Phi)]\Bigg]^2\Bigg),$$

where $Z^m_l(\Omega,\Phi) = Y^m_l e^{-i\Phi}$ is a phase-rotated spherical harmonic, Ω is the solid angle, Φ is the angle between the production and polarization planes, P_γ is the polarization magnitude, $[l]$ are the partial wave amplitudes, m is the associated m-projection, k refers to a spin flip ($k=1$) or non-flip ($k=0$) at the nucleon vertex, and κ is an overall phase space factor. The superscript $(\pm)$ denotes the reflectivity of the wave, which in our case corresponds to the naturality $\eta = P(-1)^J$ of the exchange particle assuming a t-channel production process in which a particle X is exchanged between the photon and target proton. The current data does not permit a separation between the nucleon vertex spin flip/non-flip. For this analysis, one value of k is assumed to be dominant. Parameters of the model are estimated via maximization of the model likelihood given some data. Optimization is performed by the numerical optimization library, `Minuit`. We make use of a limited waveset, including the $S^{(\pm)}_0, D^{(-)}_{-1,0,1}, D^{(+)}_{0,1,2}$ waves, guided by a model for tensor meson photoproduction [12].

Figure 2 shows the dominant D-wave contributions extracted in every bin of invariant mass for the charged and neutral channels. For $\eta\pi^0$, the a_2 signal is dominated by a contribution in the D^+_2 wave, indicating a prevalence of natural production amplitudes corresponding to ρ or ω exchange. The observation of the $a_2(1320)$ in a $m=2$ helicity state aligns with the observation of the same helicity state in $\gamma\gamma \to \eta\pi$ by the Belle Collaboration [13]. In contrast, for $\eta\pi^-$, the $a_2(1320)$ is mainly observed in a D^-_1 wave in the specified range of momentum transfer, indicating a prevalence of unnatural production amplitudes such as π exchange.

To extract the momentum-dependence of the $a_2(1320)$ photoproduction cross-section, we employed a semi-mass-independent approach to stabilize our fits, where we keep the binned formulation of the intensity for the S-wave contributions but impose a Breit-Wigner mass shape for the D-wave contributions. Figure 3 shows the preliminary result

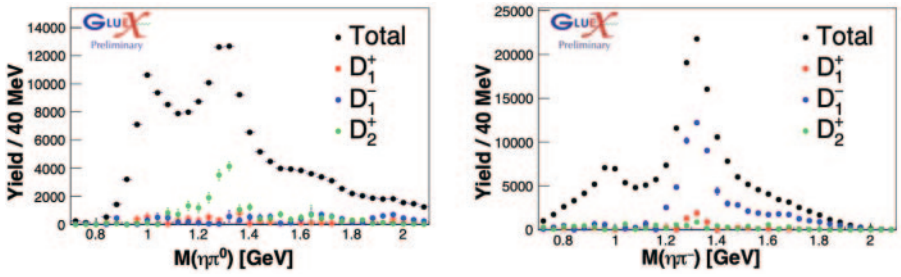

Fig. 2. – Preliminary results of a mass-independent partial wave analysis of the $\eta\pi^0$ (left) and $\eta\pi^-$ final states in the momentum transfer range of $0.1 < |-t| < 0.3\,\mathrm{GeV}^2$. Only the dominant D-wave contributions are shown to illustrate the composition especially of the $a_2(1320)$ signal.

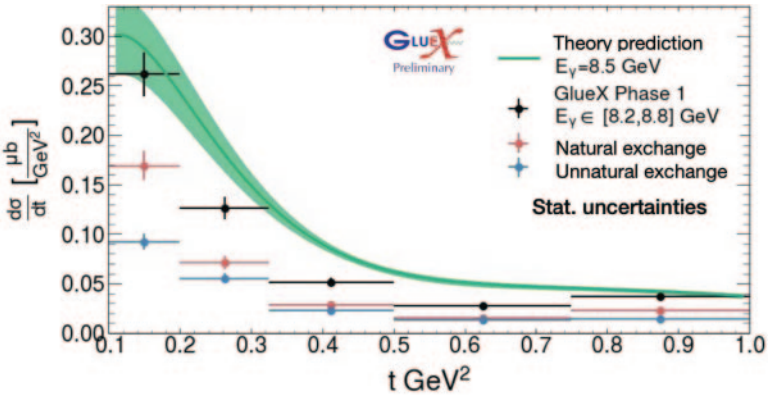

Fig. 3. – Differential photoproduction cross-section of the $a_2(1320)$ mesons in five bins of momentum transfer t extracted from a partial wave analysis of GlueX-I data allowing for the separation of the naturality of the exchange in the production process due to incorporation of the beam polarization.

for the differential cross-section in the momentum transfer range $0.1 < |-t| < 1.0\,\mathrm{GeV}^2$. We observe dominance of natural parity exchanges in the low-t region and a decent agreement with a theory prediction derived from the model referenced above [12].

3. – Projections and expectations for the $\eta'\pi$ channels

The $a_2(1320)$ signal will be used as our "standard candle" for subsequent measurements. It not only demonstrates our ability to utilize the photon polarization in an amplitude analysis, but also serves as vital input for channels in which no dominant peak is observed, but which might contain a sizeable spin-exotic contribution. We used the measured cross-section to scale an expectation for the $a_2(1320)$ contribution and project it into our invariant-mass spectrum for the $\eta'\pi$ channels (blue shaded curve in fig. 4). Furthermore, an upper limit for the photoproduction cross-section of the hybrid candidate $\pi_1(1600)$ can be derived, under the assumption that our data in the $\gamma p \to \omega\pi\pi p$

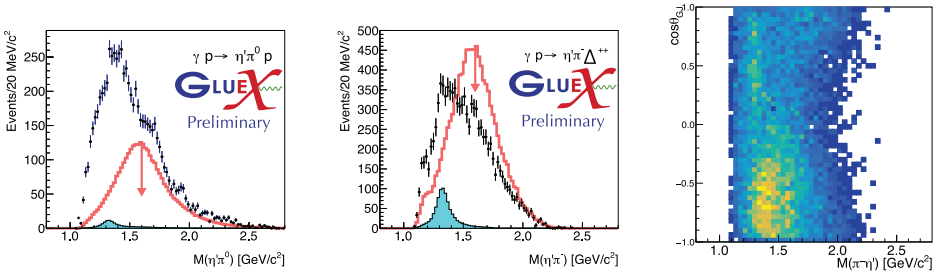

Fig. 4. – Preliminary invariant mass spectra for the $\eta'\pi^0$ (left) and $\eta'\pi^-$ (middle) final states from GlueX-I data. Points with error bars represent data, while the blue shaded curve indicates the scaled expected size of the $a_2(1320)$ contribution based on the cross-section measurement in $\eta\pi^0$. The red curve shows an upper limit projection of a spin-exotic contribution under a number of assumptions (see text). The right panel shows the polar angle of the η' in the Gottfried-Jackson frame *vs.* the $\eta'\pi^-$ invariant mass. An intriguing interference pattern in the region just below $1.5\,\mathrm{GeV}/c^2$ is observed.

channel in the mass region of the π_1 is saturated by the exotic contribution. This is motivated by Lattice QCD calculations, in which the $b_1\pi \to \omega\pi\pi$ final state is shown to be the dominant decay mode of the π_1 [14]. Using these assumptions, as well as the ratio of branching fractions to other channels (*e.g.*, $\eta'\pi$) from the same LQCD calculation and deriving the most conservative upper limit, we project this limit in the shape of a resonant contribution into the same invariant-mass spectrum (red curve in fig. 4). The resulting projections show a reasonable size of the a_2 contribution as well as the possibility for a large contribution of the π_1. Furthermore, the right panel in fig. 4 shows the polar angle of the η' in the Gottfried-Jackson frame *versus* the $\eta'\pi^-$ invariant mass. This projection of the data, although not corrected for acceptance effects, shows an intriguing, asymmetric pattern that might stem from interference effects. Forward-backward asymmetries in this projection may indicate interferences between odd- and even-J contributions.

4. – Summary

We present a detailed study of the $\eta\pi$ final states that we use to establish the foundation for hybrid meson searches in GlueX. Understanding production mechanisms as a function of $-t$ is crucial for identifying spin-exotic contributions. Preliminary results from an amplitude analysis of $\eta\pi$ final states, utilizing polarized amplitudes to determine dominant partial waves and to investigate the production mechanism, were presented. At low $-t$ natural exchanges (ρ, ω) dominate the a_2^0 production, while unnatural exchanges (π) dominate the a_2^- production. In a second step we imposed a line shape for the a_2 contribution and presented the extraction of the $-t$ dependent differential photoproduction cross-section. Finally, a projection of the expected a_2 signal as well as an upper limit for a spin-exotic π_1 contribution in the $\eta'\pi$ channels show great potential for detailed analyses of these final states in GlueX, which are underway.

* * *

Work supported by the U.S. Department of Energy, Office of Science, Office of Nuclear Physics under contract DE-AC05-06OR23177.

REFERENCES

[1] Hadron Spectrum Collaboration (Dudek J. J. *et al.*), *Phys. Rev. D*, **88** (2013) 094505.
[2] GlueX Collaboration (Adhikari S. *et al.*), *Nucl. Instrum. Methods A*, **987** (2021) 164807.
[3] GlueX Collaboration (Austregesilo A. *et al.*), these proceedings.
[4] Meyer C. A. and Swanson E. S., *Prog. Part. Nucl. Phys.*, **82** (2015) 21.
[5] JPAC Collaboration (Rodas A. *et al.*), *Phys. Rev. Lett.*, **122** (2019) 042002.
[6] GlueX Collaboration (Adhikari S. *et al.*), *Phys. Rev. C*, **103** (2021) L022201.
[7] GlueX Collaboration (Adhikari S. *et al.*), *Phys. Rev. C*, **101** (2020) 065206.
[8] GlueX Colloboration (Adhikari S. *et al.*), *Phys. Rev. C*, **100** (2019) 052201.
[9] GlueX Collaboration (Al Ghoul H. *et al.*), *Phys. Rev. C*, **95** (2017) 042201.
[10] GlueX Collaboration (Adhikari S. *et al.*), arXiv:2305.09047 [nucl-ex].
[11] JPAC Collaboration (Mathieu V. *et al.*), *Phys. Rev. D*, **100** (2019) 054017.
[12] JPAC Collaboration (Mathieu V. *et al.*), *Phys. Rev. D*, **102** (2020) 014003.
[13] Belle Collaboration (Uehara S. *et al.*), *Phys. Rev. D*, **80** (2009) 032001.
[14] Hadron Spectrum Collaboration (Woss A. J. *et al.*), *Phys. Rev. D*, **103** (2021) 054502.